Published in final edited form as:

Biomacromolecules. 2016 May 9; 17(5): 1766–1775. doi:10.1021/acs.biomac.6b00180.

Hyaluronan Hydrogels for a Biomimetic Spongiosa Layer of Tissue Engineered Heart Valve Scaffolds

Daniel S. Puperi[†], **Ronan W. O'Connell**[‡], **Zoe E. Punske**[†], **Yan Wu**[§], **Jennifer L. West**[§], and **K. Jane Grande-Allen**[*,†]

[†]Department of Bioengineering, Rice University, Houston, Texas 77005, United States

[‡]Department of Biomedical Engineering, University of Glasgow, Glasgow, United Kingdom

[§]Department of Biomedical Engineering, Duke University, Durham, North Carolina 27708, United States

Abstract

Advanced tissue engineered heart valves must be constructed from multiple materials to better mimic the heterogeneity found in the native valve. The trilayered structure of aortic valves provides the ability to open and close consistently over a full human lifetime, with each layer performing specific mechanical functions. The middle spongiosa layer consists primarily of proteoglycans and glycosaminoglycans, providing lubrication and dampening functions as the valve leaflet flexes open and closed. In this study, hyaluronan hydrogels were tuned to perform the mechanical functions of the spongiosa layer, provide a biomimetic scaffold in which valve cells were encapsulated in 3D for tissue engineering applications, and gain insight into how valve cells maintain hyaluronan homeostasis within heart valves. Expression of the HAS1 isoform of hyaluronan synthase was significantly higher in hyaluronan hydrogels compared to blank-slate poly(ethylene glycol) diacrylate (PEGDA) hydrogels. Hyaluronidase and matrix metalloproteinase enzyme activity was similar between hyaluronan and PEGDA hydrogels, even though these scaffold materials were each specifically susceptible to degradation by different enzyme types. KIAA1199 was expressed by valve cells and may play a role in the regulation of hyaluronan in heart valves. Cross-linked hyaluronan hydrogels maintained healthy phenotype of valve cells in 3D culture and were tuned to approximate the mechanical properties of the valve spongiosa layer. Therefore, hyaluronan can be used as an appropriate material for the spongiosa layer of a proposed laminate tissue engineered heart valve scaffold.

[*]***Corresponding Author:*** Tel.: +1 713 348 3704. Fax: +1 713 348 5877. grande@rice.edu.

ASSOCIATED CONTENT

Supporting Information The Supporting Information is available free of charge on the ACS Publications website at DOI: 10.1021/acs.biomac.6b00180.

Primer sequences used for qPCR; typical NMR of acrylated and methacrylated hyaluronan; method to calculate degree of modification of hyaluronan from NMR spectra; IF imaging of VICs grown in 2D with and without RGDS; hyaluronan substrate zymography controls; KIAA1199 sequenced qPCR product and results of BLAST genome search (PDF).

The authors declare no competing financial interest.

INTRODUCTION

A variety of tissue engineering strategies are being investigated to address the need for a living replacement heart valve[1] that would mitigate the limitations of currently available mechanical and bioprosthetic valves.[2,3] A tissue engineered heart valve would be constructed of a temporary biocompatible scaffold and seeded with autologous cells either in vitro or in vivo. Over time, the cells would degrade the scaffold and replace it with secreted extracellular matrix (ECM), resulting in a tissue that would ideally resemble a native heart valve in both structure and function. This goal has not yet been realized, however, as many previous attempts have resulted in leaflet contraction and fibrous tissue.[4] There is growing interest in developing a more biomimetic scaffold that will improve on previous designs by giving seeded cells local cues to direct remodeling in a way that recreates native valve architecture.[5]

Heart valves have distinct layers, distinguished by their ECM composition. On the outflow side, the fibrosa layer, which primarily consists of circumferentially aligned collagen fibers, gives the valve strength to resist the pressure gradient across the valve. The ventricularis layer is located on the inflow side of the pulmonary and aortic valves and is rich in elastic fibers. Between the fibrosa and the ventricularis is the spongiosa layer, consisting of mostly glycosaminoglycans (GAGs) and proteoglycans (PGs). The spongiosa layer provides compressive resistance during coaptation between the leaflets, lubrication between the stiffer outer layers during valve flexure, and a dampening effect on leaflet motion.[6,7] Recently, several tissue engineering approaches to design scaffolds that mimic the layered structure of the natural valve have been reported.[8–12] In this work, we examined the polymer hyaluronan with two motivations in mind: first, as a part of a broader strategy to create a layered tissue engineered heart valve scaffold; second, to better understand how valve interstitial cells (VICs) maintain hyaluronan homeostasis within the spongiosa layer of heart valves.

Hyaluronan is a naturally occurring chain of repeating disaccharides that makes up 60% of the GAGs in valve tissue.[13] Hyaluronan has been used as a substrate for studying the behavior of many different cell types in both 2D and 3D,[14] and also plays an important role in cardiac valve development.[15] Valve cells interact with hyaluronan through several different receptors and enzymes. CD44 is the primary cell surface receptor through which hyaluronan influences cells;[16] it participates in the transduction of intracellular signaling for cell proliferation, survival, and movement.[17] The receptor for hyaluronic acid-mediated motility (RHAMM or CD168) can be found in the cytosol or on the cell membrane and shares some of the same intracellular signaling pathways with CD44.[17] Cells control hyaluronan synthesis and degradation through enzymes, predominately the hyaluronan synthases HAS1, HAS2, and HAS3 and the hyaluronidases HYAL1 and HYAL2. Finally, the recently discovered protein KIA1199 has been shown to play a role in hyaluronan endocytosis and degradation. KIAA1199 was originally investigated for its role in hearing loss[18] and has been observed to be upregulated in human cancers.[19] More recently, KIAA1199 has been shown to be responsible for hyaluronan catabolism in human and mouse fibroblasts, independent of CD44 and hyaluronidase enzymes.[20,21]

To gain insight into the extent of biochemical signaling from the hyaluronan scaffold, we directly compared VIC behavior in cross-linked hyaluronan hydrogels to enzymatically degradable, but otherwise, biochemically inert, poly(ethylene glycol) diacrylate (PEGDA) hydrogels; both PEGDA and hyaluronan hydrogels have been previously investigated as 3D scaffolds for VICs.[22–30] We used these materials to evaluate hydrogels for the mechanical requirements of the spongiosa layer and to study how VICs alter expression of hyaluronan-related proteins in response to the biochemical makeup of the scaffold.

EXPERIMENTAL SECTION

Materials and Methods

All chemicals were purchased from Sigma-Aldrich (St. Louis, MO) unless indicated otherwise.

Valve Interstitial Cell Isolation and Culture

VICs were harvested from aortic valve leaflets of fresh porcine hearts obtained from a local commercial abattoir (Fisher Ham and Meats, Spring, TX) according to a validated protocol.[31] To loosen endothelial cells, dissected leaflets were digested in a collagenase 2 solution (500 U/mL, Worthington Biochemical, Lakewood, NJ) for 30 min at 37 °C. After the endothelial cells were scraped from both surfaces of the leaflets, the residual leaflet tissue was minced. The minced tissue was digested in a collagenase 3 solution (300 U/mL, Worthington Biochemical) for 4 h at 37 °C. The solution was passed through a 70 μm cell strainer and then VICs were plated in tissue culture polystyrene (TCPS) flasks. VICs were cultured in a standard humidified incubator (37 °C, 5% CO_2) in 50:50 DMEM/F12 media (Corning, Tewksbury, MA) with 10% bovine growth serum (BGS, Lonza, Walkerville, MD), 1% 1 M 4-(2-hydroxyethyl)-1-piperazineethanesulfonic acid (HEPES, Thermo Fisher Scientific, Waltham, MA), and 1% penicillin/streptomycin/ amphotericin (Corning). For consistency, all VICs were frozen after passage 1 and used in passages 2–3. VICs were used from three separate harvests with cells pooled from all aortic valve leaflets of six porcine hearts during each harvest.

PEG-Peptide Conjugation

The peptide sequence GGGPQG↓ IWGQGK (PQ) was prepared using solid phase synthesis (APEX 396, Aapptec, Louisville, KY) and verified using matrix-assisted laser desorption/ ionization time-of-flight (MALDI-TOF) mass spectrometry (Autoflex, Bruker Daltonics, Billerica, MA). RGDS peptide was purchased from American Peptide Company (Vista, CA). Acryloyl-PEG-RGDS (PEG-RGDS) and acryloyl-PEG-PQ-PEG-acryloyl (PEG-PQ) were conjugated as previously described.[25] Briefly, 3400 Da acryloyl-PEG-succinimidyl valerate (PEG-SVA, Laysan Bio, Arab, AL) was reacted with RGDS at 1:1.2 ratio or PQ at 2.1:1 ratio overnight at pH 8.0. The products were dialyzed for 48 h using a 3500 Da molecular weight cutoff dialysis membrane. Dialyzed PEG-peptide conjugates were then sterile filtered using a 0.22 μm Steriflip 50 mL tube filter (EMD Millipore, Billerica, MA), frozen, and lyophilized. Gel permeation chromatography equipped with UV and evaporative light-scattering detectors (Varian, Palo Alto, CA) was used to confirm PEG–peptide

conjugation, while proton NMR (Avance III HD 600 MHz, Bruker Daltonics) was used to confirm intact acrylate groups on the peptide-conjugated polymer.

Modification of Hyaluronan

Hyaluronan was modified with either methacrylate or acrylate groups for photoinitiated free-radical cross-linking. Hyaluronan was acrylated using a modified version of a published protocol.[32] First, 35 kDa sodium hyaluronate (NaHA, Lifecore Biomedical, Chaska, MN) underwent cation exchange (sodium to tetrabutylammonium) so that it could be dissolved in organic solvents.[33] Briefly, Dowex resin (Dowex 50WX8 H^+ form, 200–400 mesh) was washed in diH_2O before mixing with 1% w/v NaHA in water overnight at room temperature to capture the Na^+ ions. After 24 h, a Buchner funnel was used to filter the Dowex from the HA solution. The HA solution was titrated to pH 8.0 using 0.1 M tetrabutylammonium hydroxide (TBA-OH) and then lyophilized. The amount of TBA in the product was determined from proton NMR.

Acrylation of hyaluronan-tetrabutylammonium (HA-TBA) was performed under argon using acryloyl chloride (A-Cl), as shown in Scheme 1. HA-TBA (~100 mg) was dissolved in a round-bottom 3-neck flask at 1% w/v in anhydrous dimethylformamide (DMF). Anhydrous triethylamine (TEA) was added to the flask at a molar ratio of 4:1 TEA/A-Cl. The A-Cl was diluted to 10% v/v in DMF and then added to the reaction flask dropwise to achieve a final molar ratio of 0.9:1 A-Cl/(HA-TBA disaccharide). The reaction was left overnight at room temperature, protected from light. Acrylated hyaluronan (AHA) was recovered by precipitating the reaction flask contents in cold diethyl ether. The precipitate was captured by filtering in a Buchner funnel through filter paper (Whatman #3, Fisher), which was then air-dried in the dark. The filter paper with dried AHA was submerged in diH_2O for 10 min to dissolve the AHA.

Methacrylation of hyaluronan was accomplished following a previously described method with glycidyl methacrylate (GMA) in PBS[34] and depicted in Scheme 2. Either 35 or 1700 kDa NaHA (~200 mg) was dissolved at 0.375% w/v in PBS in a round-bottom flask at room temperature. TEA was added to the flask at a 7:1 TEA/(HA disaccharide) molar ratio followed by dropwise addition of GMA to a molar ratio of 14:1 GMA/(HA disaccharide). The solution was allowed to react (protected from light) for 5 days at room temperature to produce methacrylated hyaluronan (MeHA). Both MeHA and AHA solutions were dialyzed extensively against 150 mM NaCl for 3 days followed by dialysis against pure water for three additional days. The solutions were then sterile filtered and kept sterile during lyophilization and experimental use.

Hydrogel Cross-Linking and VIC Encapsulation

Sterile, lyophilized polymer was dissolved in sterile filtered photoinitiator buffer consisting of 1.5% v/v triethanolamine (TEOA), 10 μM Eosin Y, and 0.35% v/v 1-vinyl-2-pyrillidinone (NVP) in HEPES buffered saline (HBS) at 4% w/v for PEG-PQ, 2% w/v for AHA, 4% w/v for 35 kDa MeHA, and 0.75% w/v for 1700 kDa MeHA. All solutions contained 2 mM PEG-RGDS. VICs were resuspended in the photoinitiator/ polymer solution at a concentration of 15×10^6 cells/mL and cast in 5 mm diameter × 250 μm thick PDMS molds.

The gels were cross-linked under ~160 kLux of white LED light (UltraTow LED Floodlight, Northern Tool and Equipment, Burnsville, MN) for the amount of time determined from mechanical testing to produce similar stiffness hydrogels. Gels were cultured in 24 well plates in a standard humidified incubator. Encapsulated cells were grown in the same 50:50 DMEM/F12 media with 10% BGS, as described above with media changes every 2–3 days.

The LIVE/DEAD cell viability/cytotoxicity kit (Thermo Fisher Scientific) with calcein AM and ethidium homodimer-1 reagents was used to assess cell viability at days 3 and 7 after encapsulation following manufacturer instructions. Briefly, cell encapsulated gels were incubated in media with 2 μM of calcein AM and 4 μM of ethidium homodimer-1 for 30 min. Scaffolds were washed in PBS and immediately imaged on a confocal microscope (A1-Rsi, Nikon, Tokyo, Japan or LSM 510, Zeiss, Oberkochen, Germany). Live and dead cells were counted (n = 3) using Bitplane Imaris 8.2 software (Oxford Instruments, Oxfordshire, U.K.) to calculate the percentage and density of alive cells.

Mechanical Characterization of Hydrogels and Aortic Valve Tissue

All hydrogel formulations were mechanically characterized in unconfined compression. Hydrogel disks of 6 mm diameter × 0.8 mm thickness were prepared in PDMS molds and allowed to swell in PBS overnight. In order to compare response of cells to hydrogel polymer independently of stiffness, all hydrogels were made the same stiffness through an iterative process. The polymer density and cross-linking time for the hydrogels were varied and the stiffness of the gels was tested in compression. This process was repeated until all hydrogel formulations were approximately equal to the target compressive modulus of 2.5 kPa. The volume of the hydrogel disks was calculated from stereoscope images taken immediately after cross-linking the gels and again after swelling in PBS overnight. The volumetric swelling ratio was determined by dividing the increase in volume by the original hydrogel volume. Swollen gels were compressed to 30% strain using a Bose ELF 3200 mechanical tester with force measured by a 1000 g load cell (Bose ELF, Eden Prairie, MN). The compressive modulus was calculated from a linear regression of the stress versus strain plot between 5% and 15% strain. Hysteresis was determined by dividing the area between the loading and unloading stress versus strain curves by the total area under the loading curve. For comparison, aortic valve tissue (5 mm diameter cylinders cut with a biopsy punch from the belly region of aortic valve leaflets) was tested in compression using the same parameters for characterization.

Enzymatic Digest of Hydrogels

PEG-PQ and AHA hydrogels were digested in both collagenase and hyaluronidase solutions to ensure their susceptibility and specificity for enzyme activity. Hydrogel disks of 6 mm diameter × 0.8 mm thick were placed in either 50 U/mL of bovine testicular hyaluronidase (Worthington) in PBS or 10 U/mL of collagenase 3 (Worthington) in Tris buffered saline (TBS) with 2 mM $CaCl_2$ for 1, 2, 4, 12, and 24 h. Digest solution was aspirated at each time point and gels were frozen, lyophilized, and weighed. The mass of digested lyophilized gels was compared to the mass of undigested lyophilized gels.

Immunofluorescent Staining

Protein expression was visualized using immunofluorescent (IF) staining after 14 days in culture. Cells were fixed in 4% paraformaldehyde for 45 min, permeabilized in 0.25% Triton X-100 for 15 min, and blocked in 3.5% w/v bovine serum albumin (BSA) at 4 °C overnight. Primary antibodies were diluted in PBS with 1% w/v BSA and 0.05% NaN_3 and were placed on samples overnight at 4 °C. Proteins visualized via IF were αSMA (abcam ab7817; 1:50), CD44 (Calbiochem 217594; 1:120), and RHAMM (Novus NBP1–95379; 1:120). Gels were washed 4× to remove unbound primary antibody over an 8 h period in PBS with 0.01% v/v Tween 20. Secondary antibodies (AlexaFluor 488/555/633, Invitrogen Carlsbad, CA) were added at 1:200 concentration overnight at 4 °C. Samples were counterstained with DAPI and AlexaFluor 488 or 633 conjugated phalloidin (Invitrogen) for 2 h prior to imaging with a confocal microscope (Nikon A1-Rsi or Zeiss LSM 510).

RNA Isolation, qPCR, and Sequencing

Quantitative reverse transcriptase PCR (qPCR) was performed as previously described.[25] After 7 days in culture, cell-seeded hydrogels were placed in RNA lysis buffer (Zymo Research, Irvine, CA) and homogenized. mRNA was extracted with Quick-RNA MiniPrep Kit (Zymo Research) and transcribed to cDNA using a first Strand cDNA synthesis kit (Takara Bio, Otsu, Japan). The quantity and quality of mRNA was assessed using a Nanodrop 2000 UV–vis spectrophotometer (Thermo Fisher Scientific). Sample mRNA that did not have a 260/280 ratio of at least 1.8 or that was less than 5 ng/μL concentration was not transcribed to cDNA. A Mastercycler ep realplex qPCR system (Eppendorf, Hamburg, Germany) with QuantiTect SYBR Green PCR Master Mix (Clontech Laboratories, Mountain View, CA) was used to measure relative mRNA expression in VICs. Primer efficiencies and relative expression ratios were calculated using the REST 2009 program.[35] All mRNA targets and primers are listed in Supporting Information, Table S1. KIAA1199 qPCR products were purified using a QIAquick PCR purification kit (Quiagen, Venlo, Netherlands) and sequenced by Lone Star Laboratories (Houston, TX).

Gelatin and Hyaluronan Zymography

Gelatin and hyaluronan substrate zymography was performed using hand cast 10% polyacrylamide gels containing either 0.2% w/v gelatin or 0.17 mg/ mL 1700 kDa sodium hyaluronate. Protein content of conditioned media from days 11–14 of VICs cultured in PEG-PQ and AHA hydrogels was determined using the Pierce BCA total protein assay (Thermo Fisher Scientific) following manufacturer's instructions. Sample volume corresponding to 7 μg of protein was added to each well for zymography. After electrophoresis (100 V for 1 h 15 min), the polyacrylamide gels were soaked for 30 min in 2.5% Triton X-100 for renaturing and then allowed to develop overnight at 37 °C. Gelatin substrate zymography developing buffer contained 50 mM Tris, 200 mM NaCl, 5 mM $CaCl_2$, and 0.02% v/v Brij 35 at pH 7.8.[36] Parallel sets of hyaluronan substrate zymography gels were developed in either the pH 7.8 gelatin zymography developing buffer or a pH 3.0 developing buffer to detect acid-active hyaluronidases (50 mM citric acid, 50 mM dibasic sodium phosphate, 137 mM NaCl).[37] Gelatin substrate zymograms were stained for 30 min with 0.5% w/v Coomassie Blue and destained in 20% isopropanol and 10% acetic acid for 2

h. Hyaluronan substrate zymograms were stained for 1 h with 0.5% w/v Alcian Blue in 3% acetic acid and destained with 7% acetic acid for 2 h. In order to visualize protein bands in the hyaluronan substrate polyacrylamide gels, identical electrophoresis gels were stained for 20 min with Imperial Blue Stain (Thermo Fisher Scientific) and then destained in diH_2O water for 1 h. ImageJ (NIH, Bethesda, MD) was used to measure the amount of enzyme activity in the zymograms.

Statistical Methods

Single factor ANOVA with Tukey HSD posthoc analysis was performed for all comparisons of material properties. Student's t tests were used for comparison of VIC enzyme activity. qPCR data were evaluated using the pairwise fixed reallocation randomization test with the REST 2009 program. A p-value of less than 0.05 was considered significant for all tests. All results are reported as mean ± standard error of the mean.

RESULTS

Hyaluronan was Functionalized with Either Methacrylate or Acrylate Groups for Cross-Linking

Sodium hyaluronate (NaHA) was functionalized with both acrylate and methacrylate groups for photo-cross-linking, as depicted in Schemes 1 and 2, with representative resultant ^1H NMR spectra shown in Supporting Information, Figure S1. Hyaluronan acrylation was consistent and repeatable with 7.2 ± 0.7% (n = 12) degree of modification (DOM) for the reaction conditions used. Low (35 kDa) and high (1700 kDa) molecular weight hyaluronan were methacrylated with 2.6 ± 0.1% (n = 2) and 2.1% (n = 1) DOM, respectively. Details of DOM calculations are provided in the Supporting Information. High molecular weight NaHA was not successfully ion exchanged to a HA-TBA salt that was soluble in DMF, and therefore was functionalized with methacrylate groups in an aqueous solution.

Hyaluronan Hydrogel Mechanical Properties Can Be Optimized for a Spongiosa Layer Mimic

Cross-linked hydrogels were characterized by unconfined compression testing. The compressive modulus of valve tissue dissected from the belly region of aortic leaflets was 5.13 ± 0.36 kPa (n = 24), which served as an approximate target elastic modulus for hydrogels. Hydrogel weight fraction and cross-linking time under ~160 kLux of white light were varied to achieve a similar modulus among materials so that the biochemical results were independent of the substrate stiffness. The resulting mechanical characteristics of the hydrogels are shown in Table 1 and Figure 1. PEG-PQ, AHA, and 35 kDa MeHA hydrogels were all prepared to have approximately 2.7 kPa compressive modulus. It was not possible to prepare 1700 kDa MeHA hydrogels to achieve an elastic modulus greater than 1.6 kPa: increasing cross-linking time above 120 s had no effect and increasing weight percent over 0.75% made cell encapsulation difficult due to high viscosity at 37 °C. In order to provide a comparison between 1700 kDa MeHA and PEG-PQ hydrogels of similar stiffness, PEG-PQ was also formulated with less cross-linking time (t = 22 s) to produce a weaker hydrogel. The 1700 kDa MeHA and soft PEG-PQ hydrogels were significantly less stiff than other formulations (n = 5; $p < 0.01$).

The hysteresis of valve leaflets in compression was 64.9 ± 2.2% (n = 24). As shown in Table 1 and Figure 1B, hysteresis of the 1700 kDa MeHA and softer PEG-PQ hydrogels was significantly higher than all other materials ($p < 0.01$; Figure 1B). Hysteresis of the AHA hydrogel was greater than that of the PEG-PQ and 35 kDa MeHA, despite having similar compressive moduli ($p < 0.01$). The volumetric swelling of the hydrogels after cross-linking was calculated to determine how well hydrogels would retain their molded dimensions. The 1700 kDa MeHA hydrogels swelled significantly less and 35 kDa MeHA hydrogels swelled significantly more that PEG-PQ and AHA hydrogels ($p < 0.01$; Figure 1C). Because of the 2× greater swelling in 35 kDa MeHA hydrogels, they were not used for cell encapsulation. MeHA refers to 1700 kDa MeHA throughout the remainder of this study.

Finally, hydrogels were digested in exogenous enzymes to verify the specificity of their degradation mechanism (Figure 1D). PEG-PQ hydrogels quickly degraded over a 4 h period when subject to collagenase but were unaffected by hyaluronidase for up to 24 h. Hyaluronan hydrogels were degraded with hyaluronidase but were unaffected by collagenase over the same time periods.

Hyaluronan Hydrogels Support 3D Culture of VICs with the RGDS Cell-Adhesive Ligand

VICs were first grown in 2D atop of PEG-PG and AHA hydrogels to determine if RGDS integrin ligand was required. Neither PEG-PQ and AHA scaffolds without PEG-RGDS supported strong VIC attachment as VICs formed round clusters of cells on the surface of the hydrogels after 7 days in culture (Supporting Information, Figure S2A,B). VICs readily adhered in 2D to PEG-PQ and hyaluronan scaffolds that had PEG-RGDS present for cell attachment after 7 days in culture (Supporting Information, Figure S2C–E). Therefore, when VICs were encapsulated in 3D, all scaffold materials contained 2 mM PEG-RGDS, and the healthy, spread morphology of VICs was evident and similar in all materials for at least 14 days in culture (Figure 2A,B).

Expression of VIC activation marker αSMA expression was low in all hydrogel formulations as demonstrated through qPCR and IF staining (Figure 2C,D). The only location on hydrogels where strong αSMA stress fiber staining was observed was on the surface of the gels (Figure 2E). As expected, αSMA gene expression of VICs cultured on TCPS was significantly higher than for VICs encapsulated in all hydrogel formulations (n = 16 TCPS, 9 AHA, 11 PEG-PQ, 8 MeHA, 4 soft PEG-PQ; $p < 0.01$; Figure 2F). VICs in MeHA and soft PEG-PQ also had significantly lower αSMA gene expression than did VICs in the stiffer PEG-PQ hydrogels ($p < 0.01$).

VICs demonstrated greater than 80% viability in PEG-PQ, AHA, and MeHA hydrogels, as shown by LIVE/DEAD staining after 3 and 7 days in 3D culture (Figure 3). Cells were more spread after 7 days, but cell numbers were not statistically different from day 3 to day 7. At day 7, the cell density is significantly higher ($p < 0.05$) in the MeHA hydrogels than in the AHA and PEG-PQ hydrogels (Figure 3H), but that is attributed to the faster hydrogel degradation, which resulted in lower imaged volume because the z-stack size was only 150 μm compared to 200 μm for AHA and PEG-PQ samples.

VICs Alter Hyaluronan-Related Gene Expression in Response to Hyaluronan Hydrogels

VICs expressed similar, very strong levels of CD44 in all hydrogel formulations (Figure 4A,B). In contrast, VICs had very little RHAMM protein, showing only diffuse intracellular IF staining in all hydrogels (Figure 4C). qPCR was used to measure gene expression of CD44 and the hyaluronan synthases HAS1, HAS2, and HAS3 (Figure 4E–H; CD44 n = 12 TCPS, 16 AHA, 11 PEG-PQ, 8 MeHA; HAS1–3 n = 8 TCPS, 8 AHA, 5 PEG–PQ, 8 MeHA). There were no significant differences in gene expression of CD44 and HAS2 between scaffold materials. HAS1 gene expression was significantly higher in VICs cultured in AHA than in PEG-PQ or on TCPS ($p < 0.01$). VICs in PEG-PQ hydrogels had significantly higher HAS3 expression than VICs in MeHA hydrogels ($p < 0.05$).

KIAA1199 Protein is Expressed in VICs

KIAA1199 gene expression was confirmed through qPCR in VICs grown in 2D on TCPS and 3D in PEG-PQ and hyaluronan hydrogels. KIAA1199 gene expression was significantly less in the MeHA and soft PEG-PQ hydrogels than on TCPS (Figure 4D; n = 6 TCPS, 8 AHA, 9 PEG-PQ, 8 MeHA, 4 soft PEG-PQ; $p < 0.01$). The DNA sequence of qPCR products from VICs cultured on TCPS using the forward KIAA1199 primer is shown in Supporting Information, Figure S3A. A BLAST search of the sequenced qPCR product in the Sus scrofa genome confirmed predicted KIAA1199 nucleotide sequences (Supporting Information, Figure S3B).

VIC Enzyme Activity Remains Consistent across Hydrogel Material

Gelatin substrate and hyaluronan substrate zymography were used to identify enzyme activity of VICs encapsulated in hydrogels. VICs did not change their secreted gelatinase (MMP2 and MMP9) or hyaluronidase enzyme profile when cultured in either PEG-PQ or AHA hydrogels, as evidenced by zymogram band intensity (Figure 5A–D). Controls ensured that the clear bands observed in the hyaluronan substrate zymograms were from cell secreted hyaluronidase activity (Supporting Information, Figure S4). VICs cultured in media without serum secreted hyaluronidase enzymes that were active on the hyaluronan substrate at pH 3.0 (Supporting Information, Figure S4A). While some of the observed enzyme activity is from hyaluronidase in the serum, hyaluronidase activity was also observed without serum in the media. Another potential problem was that protein may have been blocking alcian blue from staining the electrophoresis gel. To investigate that possibility, gels were developed at neutral pH. Protein bands were present at ~50 kDa in both acidic and neutral pH cases, but the enzymes were not active at pH 7.8 and did not prevent alcian blue from staining the hyaluronan substrate (Supporting Information, Figure S4B). Bovine testicular hyaluronidase controls were active at pH 7.8.

Gene expression of hyaluronidase-1 (HYAL1), hyaluronidase-2 (HYAL2), and MMP-2 enzymes from VICs cultured in different hydrogels were compared using qPCR (Figure 5E–G). MMP-2 gene expression was significantly higher in VICs cultured in PEG-PQ hydrogels than TCPS or MeHA substrates (Figure 5E; n = 5 TCPS, 8 AHA, 5 PEG-PQ, 8 MeHA; $p < 0.01$). There was no significant difference in HYAL1 expression between VICs grown on any substrate (Figure 5E; n = 12 TCPS, 13 AHA, 13 PEG-PQ, 8 MeHA; $p > 0.8$), which was consistent with zymography results. There was significantly lower HYAL2 gene expression

in VICs grown on TCPS compared to VICs grown in PEG-PQ or MeHA hydrogels (Figure 5F; $p < 0.01$).

DISCUSSION

The layered structure of the ECM in natural heart valves has led engineers toward a layering approach to construct a biomimetic tissue engineered valve scaffold.[9–12] In this study, hyaluronan hydrogels were utilized to represent the GAG-rich spongiosa layer of heart valves as part of a broader layering strategy. Hyaluronan was functionalized with acrylate (Scheme 1) and methacrylate (Scheme 2) groups to allow for photoinitiated free-radical polymerization, which was well tolerated by encapsulated cells (Figures 2 and 3). The mechanical properties of the hydrogels were successfully tuned to approximate both the mechanical properties and function of the spongiosa layer in the heart valve leaflet. To gain insight into the degree of biochemical signaling from the cross-linked hyaluronan scaffold, we studied behavior of VICs encapsulated in hyaluronan hydrogels compared to PEG-PQ hydrogels. Throughout the study, VICs demonstrated very similar behavior in both hyaluronan and PEG-PQ hydrogels. Similar levels of CD44 expression, KIAA1199 expression, and hyaluronidase enzyme activity were observed in both materials. Results from gene expression analysis of the three isoforms of hyaluronan synthase enzymes showed that HAS1 expression was upregulated in AHA hydrogels, whereas HAS2 and HAS3 expression were similar in AHA and PEG-PQ. Overall, the results of this study demonstrate that hyaluronan hydrogels can be tuned for the mechanical purpose of building complex tissue engineering scaffolds and can provide insight into the extent of biochemical signaling to encapsulated cells from cross-linked hyaluronan hydrogels.

The goal of this study was to compare behavior of VICs encapsulated in photo-cross-linked AHA versus PEG-PQ scaffold materials. Hyaluronan was functionalized at a low DOM to retain as much biological activity from the hyaluronan as possible. Seven percent DOM from the acrylation reaction resulted, on average, in one of every 14.3 disaccharides with a vinyl group, corresponding to ~5400 Da of hyaluronan disaccharide between cross-links, independent of the molecular weight of the sodium hyaluronate used in the reaction. The 7% DOM is lower than reported DOM for other studies of VICs encapsulated in hyaluronan hydrogels.[22,28] Because very little difference was observed between AHA and PEG-PQ scaffolds, hyaluronan was also methacrylated with only 2% DOM in order to maximize the biological availability of hyaluronan to encapsulated cells. The 2% DOM corresponds to having 1 in every 50 disaccharides functionalized or about 19000 Da of hyaluronan between cross-links. Additionally, larger molecular weight hyaluronan is more representative of the physiological molecule.[38] The acrylation reaction did not have fine enough control to target 2%, and we could not ion exchange 1700 kDa NaHA to a HA-TBA product that was soluble in DMF. Therefore, methacrylation was used to synthesize a cross-linkable hyaluronan molecule that most closely resembles the hyaluronan found in the natural heart valve (large molecular weight = 1700 kDa, low cross-linking density = 2% DOM).

The mechanical properties of photo-cross-linked hyaluronan hydrogels were comparable to native valve tissue. The bulk compressive modulus of the aortic valve leaflet was measured to be 5.13 ± 0.36 kPa, but this value includes compressive resistance of all three layers. Few

studies have isolated the mechanical properties of the spongiosa layer; a recently published report used atomic force microscopy to approximate Young's modulus of the spongiosa layer to be in the 4–8 kPa range.[39] We targeted the compressive modulus of the hyaluronan and PEGDA hydrogels to be between 2 and 3 kPa by varying polymer concentration and cross-linking time. The stiffness value was chosen based on our bulk compressive measurements of the whole leaflet, capabilities of the polymers that we were using, and comparison to previously published work that used hyaluronan hydrogels for VIC culture.[22] The 1700 kDa MeHA hydrogels were unable to be cross-linked to stiffnesses greater than ~1.6 kPa at 0.75% w/v. The 1700 kDa MeHA hydrogels could theoretically have been made more stiff with higher weight percentage of the polymer, but at higher weight percentage, the liquid was too viscous at physiological temperatures to be used effectively for cell encapsulation. PEG-PQ hydrogels that matched the compressive modulus of the 1700 kDa MeHA were constructed in order to determine if differences seen in VIC behavior encapsulated the 1700 kDa MeHA scaffolds were a result of bulk stiffness or due to the biochemical signaling from the hyaluronan scaffold.

Both 1700 kDa MeHA and AHA had significantly higher hysteresis than PEG-PQ and 35 kDa MeHA and in the range of the measured 64.9% hysteresis of valve leaflets. The mechanical function of hyaluronan in the heart valve is one of lubrication and dampening.[6,7] Scaffolds with an increased level of hysteresis would serve these functions well, as hysteresis is a measure of energy dissipation. Therefore, either AHA or 1700 kDa MeHA would be appropriate materials to match the dampening function of the spongiosa layer. The proposed goal of lamination of the spongiosa hydrogel with other scaffold materials requires that the spongiosa layer swelling be minimized to prevent possible delamination and/or unnatural force distribution in the trilaminate scaffold. The 1700 kDa MeHA swelling was significantly less than the AHA or PEG-PQ materials, despite having lower DOM and compressive modulus. The reduced swelling is a result of the higher molecular weight of the hyaluronan molecule. Despite the same 2% DOM as the 1700 kDaA MeHA, the 35 kDa MeHA hydrogels had significantly greater swelling than had all other materials, rendering it unsuitable for a laminated heart valve scaffold prepared using our previously reported lamination strategy.[12] Therefore, all following biological studies (zymography, qPCR, IF) did not use 35 kDa MeHA. Overall, the mechanical properties of the 2% DOM 0.75% w/v 1700 kDa MeHA appear to be the best at supporting the mechanical requirements of the spongiosa layer. However, when VICs were cultured in 3D, the 1700 kDa MeHA scaffold degraded after only about 2 weeks. In comparison, the PEG-PQ and AHA hydrogels did not fully degrade for at least 4 weeks in culture.

VICs seeded in 2D atop both hyaluronan and PEG-PQ hydrogels without the RGDS peptide confirmed previous research showing that VICs require integrin ligands to attach to hydrophilic cross-linked scaffolds.[22,25] Without RGDS, any viable VICs retained rounded morphology and clumped together rather than spread on the substrate (Supporting Information, Figure S2A,B). Therefore, all hydrogel formulations used for encapsulation contained 2 mM of PEG-RGDS for integrin binding. VICs were encapsulated throughout the hyaluronan scaffold during photo-cross-linking so that the cells did not need to adopt an invasive, disease-like phenotype in order to populate the interior of the scaffold.

Immunofluorescent imaging and qPCR analysis demonstrated the relative expression of hyaluronan related proteins in VICs grown in 3D hydrogel culture. Hyaluronan-binding cell surface receptor CD44 was strongly present in VICs in either PEG-PQ or hyaluronan hydrogel scaffolds (Figure 4A,B). qPCR confirmed similar expression levels of the CD44 gene, regardless of scaffold material (Figure 4E). Hyaluronan synthase gene expression was also very similar between hydrogel formulations, but interestingly HAS1 was upregulated in VICs cultured in AHA hydrogels compared to PEG-PQ hydrogels (Figure 4F). While HAS2 has been studied in valves and is known to be required for proper valve development,[40] there are no previously published reports of HAS1 expression in valve cells or tissue. In other types of fibroblasts, inflammatory factors IL-1β and TGF-β, as well as glycemic stress, have been shown to cause upregulation of HAS1 expression.[41–43] HAS1 has also been implicated in malignant transformation of several types of cancer.[44,45] Encapsulated VICs break down the scaffold as they elongate and migrate; the resulting cleaved hyaluronan fragments may induce an inflammatory response,[46,47] as evidenced by upregulation of HAS1 in the AHA scaffold. Based on these results, further research into the VIC inflammatory response due to breakdown of cross-linked hyaluronan scaffolds is warranted.

This study confirmed the expression of the hyaluronan binding and depolymerizing peptide KIAA1199 in porcine aortic VICs. KIA1199 was studied in order to investigate another possible mechanism of hyaluronan binding and degradation in light of the weak hyaluronidase activity that was observed in zymography. KIAA1199 has been investigated in hearing loss,[18] cancers,[19] and dermal fibroblasts[20] of humans, but has not been studied in porcine cells or in heart valves of any species. We have shown through qPCR that KIAA1199 is expressed in porcine aortic VICs (Figure 4D). The biological significance and role of KIAA1199 in valve cell and tissue function is still unknown, but our data suggests that less stiff substrates downregulate the expression of KIAA1199. For the least stiff scaffolds (1700 kDa MeHA and soft PEG-PQ) KIAA1199 gene expression was significantly less than it was for TCPS. Future work will be needed to demonstrate how porcine KIAA1199 is involved in hyaluronan catabolism in valve cells.

Although we had hypothesized that VICs would respond to the hydrogel scaffold by upregulating the enzymes that would degrade each scaffold material, zymography confirmed similar enzyme activity between VICs independent of substrate polymer makeup (Figure 5A–D). The gelatin substrate zymogram showed strong MMP2 activity, while the hyaluronan substrate zymogram had bright bands at ~52 kDa, corresponding to hyaluronidase 1, which is known to be activated at an acidic pH.[46] Hyaluronidase 2 was not expected to be detected in conditioned media as it is tethered to the cell membrane by glycosylphosphatidyl-inositol.[46] The zymograms also demonstrate that overall MMP activity was much stronger than hyaluronidase activity per mass of total protein from the conditioned media. Although the expression of hyaluronidase genes (HYAL1 and HYAL2) was the same between AHA and PEG-PQ hydrogels, mRNA expression of MMP2 was significantly higher in PEG-PQ hydrogels (Figure 5E–G), indicating some ability of the cells to control enzyme activity appropriate for the PEG-PQ scaffold. However, MMP activity is also heavily regulated by other enzymes, including tissue inhibitors of metalloproteinases (TIMPs), therefore, MMP2 gene expression is a less complete description of enzyme activity than the zymography results.

The results of this study showed only subtle differences in VIC behavior between the AHA and PEG-PQ hydrogels, but previous research has shown that scaffold design has a noticeable effect on VIC behavior. For instance, substrate stiffness is known to play a role in VIC response to the scaffold,[22] and VICs are highly dependent on integrin ligands for healthy, spread phenotype.[30,48,49] To control these factors, we designed scaffolds from different materials, while maintaining consistent stiffness and PEG-RGDS concentration. The corresponding consistency in our results may indicate that stiffness and adhesive ligand presentation are the most influential factors to guide VIC behavior, rather than the specific material substrate. Furthermore, although hyaluronan DOM was targeted to be low (7 or 2%), cross-linking may still have rendered the hyaluronan hydrogel biochemical inert to hyaluronan receptors. Research has demonstrated that CD44-hyaluronan interactions are a multivalent process, requiring large fragments of hyaluronan and clustering of CD44 to maintain the bound state.[50,51] The results of this study suggest that cross-linked hyaluronan scaffolds, at even lower DOM, may render the hyaluronan unavailable for the complex interactions necessary to bind with CD44.

Although we have proposed using hyaluronan hydrogels as part of a tissue engineered heart valve scaffold, these results presented here should be interpreted in the appropriate context. To begin, all data was acquired from statically cultured samples, without applied mechanical stimulation. Heart valves normally experience cyclic tension, shear, compression, and bending forces continuously throughout their lifetime, so understanding how cells in the spongiosa layer react to physiologically relevant forces and motion is an important research goal. While hyaluronan makes up 60% of the GAGs in valve tissue, the natural valve spongiosa layer also contains other important biological molecules, such as sulfated GAGs, proteoglycans, and elastic fibers.[52] A scaffold intended to mimic all of the key biochemical features of the spongiosa layer would need to account for this additional complexity. Additionally, previous research found increased elastin secretion by VICs in hyaluronan scaffolds with the addition of exogenous hyaluronidase enzymes, small hyaluronan fragments, or culture times of up to 6 weeks.[24,26,28] We were not able replicate these results without addition of exogenous factors, although in this study VICs were only cultured for up to 4 weeks.

Finally, although we investigated several hyaluronan hydrogel formulations, there still remain opportunities to identify whether modulating a combination of polymer functionalization, DOM, stiffness, RGDS concentration, and hydrogel weight fraction can significantly alter VIC behavior in the hydrogels. Strategies to make the hyaluronan backbone or digested hyaluronan fragments more available for cellular processing may lead to changes in cell signaling from the scaffold material. The mechanical properties of the AHA and PEG-PQ scaffolds were fine-tuned by modulating cross-linking time. However, under-cross-linking will leave free acrylate groups in the hydrogel. While the acrylate groups are unlikely to affect cell viability,[53] they may react with biological molecules and in turn have an effect on cell behavior in an unpredictable manner. To mitigate this possibility, mechanical properties could also be adjusted by changing the polymer weight fraction, but we had better fine control over final compressive modulus by changing cross-linking time, rather than polymer weight fraction.

CONCLUSIONS

Photo-cross-linked hyaluronan hydrogels were investigated for use in a layered, synthetic, tissue-engineered heart valve. The mechanical properties of hyaluronan-based hydrogels were tuned to match the mechanical purposes of the valve spongiosa layer. VICs cultured in hyaluronan demonstrated only subtle differences compared to those cultured in PEG-based scaffolds. These results suggest that factors such as scaffold stiffness or RGDS integrin ligand concentration may be far more influential than hydrogel polymer formulation for directing VIC behavior. However, the results may also suggest that cross-linking the hyaluronan renders it less biochemically available for cell signaling. In either case, cross-linked hyaluronan was shown to be a tunable scaffold material that promotes the quiescent, healthy phenotype of VICs in 3D culture and can be used as part of a broader layering strategy for heart valve tissue engineering.

Supplementary Material

Refer to Web version on PubMed Central for supplementary material.

Acknowledgments

This work was funded by a National Science Foundation Graduate Research Fellowship (to D.S.P.) and a National Institutes of Health Grant R01HL107765. The authors would like to thank the Drezek lab at Rice University for generous sharing of equipment, Dr. Shauna Dorsey from Dr. Jason Burdick's lab at University of Pennsylvania for consultation regarding HA-TBA synthesis, Dr. Melanie Simpson from University of Nebraska-Lincoln for consultation regarding hyaluronidase activity, and Drs. Eliza Fong and Brian Grindel from the Farach-Carson lab at Rice University for supplying C4-2 cells and conditioned media. The authors would also like to thank Dr. Jennifer Connell for editorial assistance with the manuscript.

REFERENCES

1. Cheung DY, Duan B, Butcher JT. Expert Opin. Biol. Ther. 2015; 15:1–18. [PubMed: 25323456]
2. Zilla P, Brink J, Human P, Bezuidenhout D. Biomaterials. 2008; 29(4):385–406. [PubMed: 17950840]
3. Sewell-Loftin MK, Chun YW, Khademhosseini A, Merryman WDJ. Cardiovasc. Transl. Res. 2011; 4:658–671.
4. Vesely I. Circ. Res. 2005; 97(8):743–755. [PubMed: 16224074]
5. Butcher JT, Mahler GJ, Hockaday LA. Adv. Drug Delivery Rev. 2011; 63(4–5):242–268.
6. Eckert CE, Fan R, Mikulis B, Barron M, Carruthers Ca, Friebe VM, Vyavahare NR, Sacks MS. Acta Biomater. 2013; 9(1):4653–4660. [PubMed: 23036945]
7. Buchanan RM, Sacks MS. Biomech. Model. Mechanobiol. 2014; 13(4):813–826. [PubMed: 24292631]
8. Simionescu DT, Chen J, Jaeggli M, Wang B, Liao JJ. Healthc. Eng. 2012; 3:179–202.
9. Tedder ME, Simionescu A, Chen J, Liao J, Simionescu DT. Tissue Eng., Part A. 2011; 17(1–2):25–36. [PubMed: 20673028]
10. Masoumi N, Annabi N, Assmann A, Larson BL, Hjortnaes J, Alemdar N, Kharaziha M, Manning KB, Mayer JE, Khademhosseini A. Biomaterials. 2014; 35(27):7774–7785. [PubMed: 24947233]
11. Jahnavi S, Kumary TV, Bhuvaneshwar GS, Natarajan TS, Verma RS. Mater. Sci. Eng. C. 2015; 51:263–273.
12. Tseng H, Cuchiara ML, Durst CA, Cuchiara MP, Lin CJ, West JL, Grande-Allen KJ. Ann. Biomed. Eng. 2013; 41:398. [PubMed: 23053300]
13. Grande-Allen KJ, Osman N, Ballinger ML, Dadlani H, Marasco S, Little PJ. Cardiovasc. Res. 2007; 76(1):19–28. [PubMed: 17560967]

14. Burdick JA, Prestwich GD. Adv. Mater. 2011; 23(12):41–56.
15. Armstrong EJ, Bischoff J. Circ. Res. 2004; 95:459–470. [PubMed: 15345668]
16. Aruffo A, Stamenkovic I, Melnick M, Underhill CB, Seed B. Cell. 1990; 61(7):1303–1313. [PubMed: 1694723]
17. Toole BP. Nat. Rev. Cancer. 2004; 4(7):528–539. [PubMed: 15229478]
18. Abe S, Usami SI, Nakamura YJ. Hum. Genet. 2003; 48(11):564–570.
19. Tiwari A, Schneider M, Fiorino A, Haider R, Okoniewski MJ, Roschitzki B, Uzozie A, Menigatti M, Jiricny J, Marra G. PLoS One. 2013; 8(7):e69473. [PubMed: 23936024]
20. Yoshida H, Nagaoka A, Kusaka-Kikushima A, Tobiishi M, Kawabata K, Sayo T, Sakai S, Sugiyama Y, Enomoto H, Okada Y, Inoue S. Proc. Natl. Acad. Sci. U. S. A. 2013; 110(14):5612–5617. [PubMed: 23509262]
21. Yoshida H, Nagaoka A, Nakamura S, Sugiyama Y, Okada Y, Inoue S. FEBS Open Bio. 2013; 3:352–356.
22. Duan B, Hockaday LA, Kapetanovic E, Kang KH, Butcher JT. Acta Biomater. 2013; 9(8):7640–7650. [PubMed: 23648571]
23. Eslami M, Vrana NE, Zorlutuna P, Sant S, Jung S, Masoumi N, Khavari-Nejad RA, Javadi G, Khademhosseini AJ. Biomater. Appl. 2014; 29:399–410.
24. Masters KS, Shah DN, Leinwand LA, Anseth KS. Biomaterials. 2005; 26(15):2517–2525. [PubMed: 15585254]
25. Puperi DS, Balaoing LR, O'Connell RW, West JL, Grande-Allen KJ. Biomaterials. 2015; 67:354–364. [PubMed: 26241755]
26. Ramamurthi A, Vesely I. Biomaterials. 2005; 26(9):999–1010. [PubMed: 15369688]
27. Rodriguez KJ, Piechura LM, Masters KS. Matrix Biol. 2011; 30(1):70–82. [PubMed: 20884350]
28. Shah DN, Recktenwall-Work SM, Anseth KS. Biomaterials. 2008; 29(13):2060–2072. [PubMed: 18237775]
29. Wang H, Tibbitt MW, Langer SJ, Leinwand LA, Anseth KS. Proc. Natl. Acad. Sci. U. S. A. 2013; 110(48):19336–19341. [PubMed: 24218588]
30. Gould ST, Anseth KSJ. Tissue Eng. Regener. Med. 2013 n/a.
31. Stephens EH, Carroll JL, Grande-Allen KJJ. Heart Valve Dis. 2007; 16(2):175–183.
32. Wang X, Messman J. Biomacromolecules. 2010; 11(9):2313–2320. [PubMed: 20690642]
33. Khetan S, Burdick JA. Biomaterials. 2010; 31(32):8228–8234. [PubMed: 20674004]
34. Bencherif, Sa; Srinivasan, A.; Horkay, F.; Hollinger, JO.; Matyjaszewski, K.; Washburn, NR. Biomaterials. 2008; 29(12):1739–1749. [PubMed: 18234331]
35. Pfaffl MW, Horgan GW, Dempfle L. Nucleic Acids Res. 2002; 30(9):e36. [PubMed: 11972351]
36. Toth M, Sohail A, Fridman R. Methods Mol. Biol. 2012; 878:121–135. [PubMed: 22674130]
37. Simionescu DT, Lovekamp JJ, Vyavahare NRJ. Heart Valve Dis. 2003; 12:217–225.
38. Fraser JR, Laurent TC, Laurent UBJ. Intern. Med. 1997; 242:27–33.
39. Hinderer S, Seifert J, Votteler M, Shen N, Rheinlaender J, Schaffer TE, Schenke-Layland K. Biomaterials. 2014; 35(7):2130–2139. [PubMed: 24333025]
40. Camenisch TD, Spicer AP, Brehm-Gibson T, Biesterfeldt J, Augustine ML, Calabro A, Kubalak S, Klewer SE, McDonald JAJ. Clin. Invest. 2000; 106(3):349–360.
41. Siiskonen H, Karna R, Hyttinen JM, Tammi RH, Tammi MI, Rilla K. Exp. Cell Res. 2014; 320(1):153–163. [PubMed: 24099991]
42. Meran S, Thomas D, Stephens P, Martin J, Bowen T, Phillips A, Steadman RJ. Biol. Chem. 2007; 282(35):25687–25697.
43. Chen L, Neville RD, Michael DR, Martin J, Luo DD, Thomas DW, Phillips AO, Bowen T. Matrix Biol. 2012; 31(7–8):373–379. [PubMed: 23123404]
44. Itano N, Sawai T, Atsumi F, Miyaishi O, Taniguchi S, Kannagi R, Hamaguchi M, Kimata KJ. Biol. Chem. 2004; 279(18):18679–18687.
45. Golshani R, Lopez L, Estrella V, Kramer M, Iida N, Lokeshwar VB. Cancer Res. 2008; 68(2):483–491. [PubMed: 18199543]
46. Girish KS, Kemparaju K. Life Sci. 2007; 80:1921–1943. [PubMed: 17408700]

47. Turley, Ea; Noble, PW.; Bourguignon, LYWJ. Biol. Chem. 2002; 277(7):4589–4592.
48. Benton JA, Fairbanks BD, Anseth KS. Biomaterials. 2009; 30(34):6593–6603. [PubMed: 19747725]
49. Zhang X, Xu B, Puperi DS, Yonezawa AL, Wu Y, Tseng H, Cuchiara ML, West JL, Grande-Allen KJ. Acta Biomater. 2015; 14:11–21. [PubMed: 25433168]
50. Wolny PM, Banerji S, Gounou C, Brisson AR, Day AJ, Jackson DG, Richter RPJ. Biol. Chem. 2010; 285(39):30170–30180.
51. Banerji S, Wright AJ, Noble M, Mahoney DJ, Campbell ID, Day AJ, Jackson DG. Nat. Struct. Mol. Biol. 2007; 14(3):234–239. [PubMed: 17293874]
52. Tseng H, Grande-Allen KJ. Acta Biomater. 2011; 7(5):2101–2108. [PubMed: 21255691]
53. Yoshii EJ. Biomed. Mater. Res. 1997; 37(4):517–524.

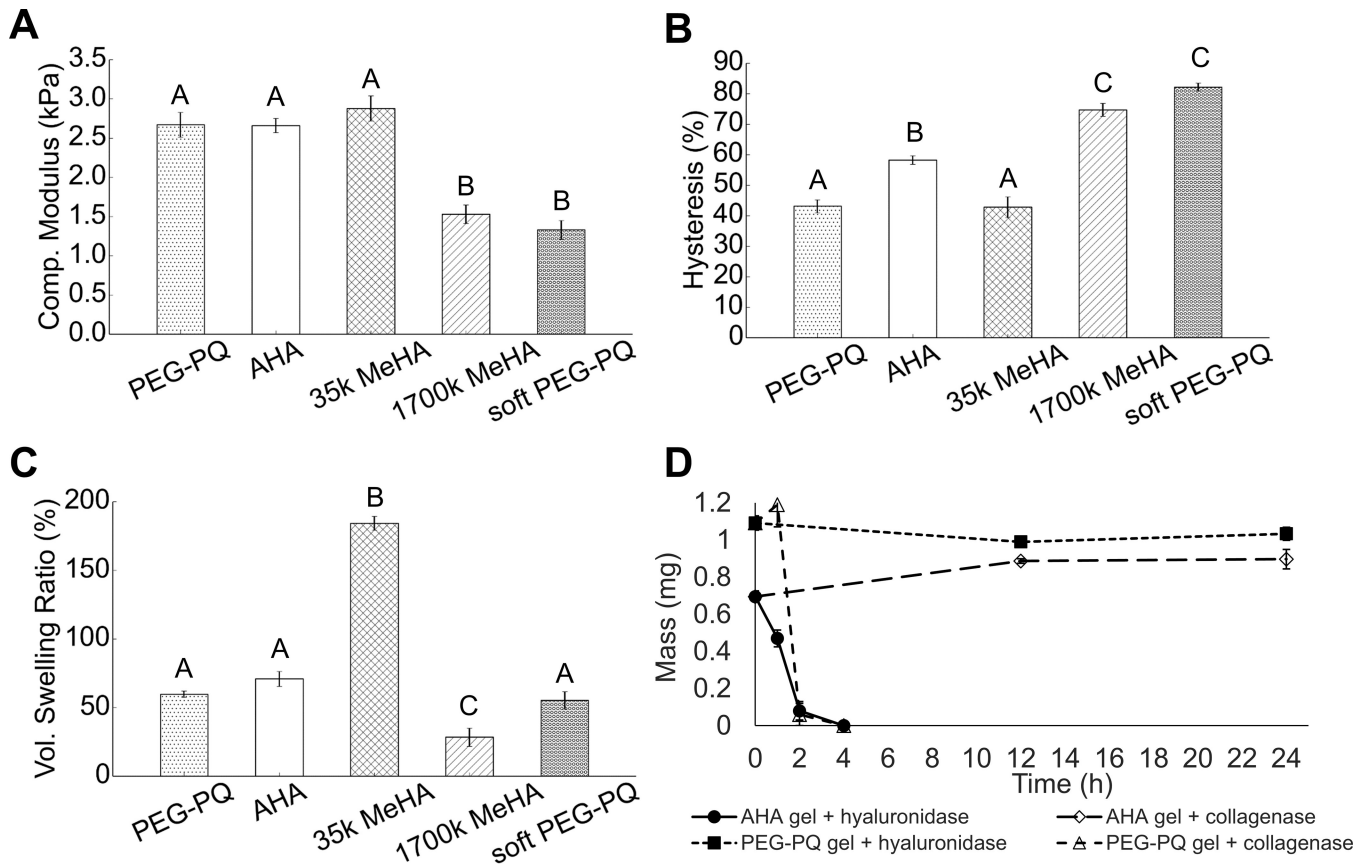

Figure 1.

Mechanical characterization of cross-linked hydrogels. (A) Bulk compressive modulus of PEG-PQ and hyaluronan variants. 1700 kDa MeHA and soft PEG-PQ had significantly lower compressive modulus than others ($p < 0.01$). (B) Hysteresis during compression; 1700 kDa MeHA, soft PEG-PQ and AHA had significantly greater hysteresis than others with 1700 kDa MeHA and soft PEG-PQ significantly higher than AHA ($p < 0.01$). (C) Volumetric swelling ratio overnight in PBS demonstrates dimensional change after cross-linking. Swelling for the 35 kDa MeHA was significantly greater than all others ($p < 0.01$); swelling for the 1700 kDa MeHA was significantly less than all others ($p < 0.05$; bars that do not share a common letter are statistically different from each other). (D) Lyophilized mass of enzyme-digested hydrogels over 24 h demonstrated susceptibility and specificity of PEG-PQ and AHA hydrogels to collagenase and hyaluronidase. Collagenase degraded only PEG-PQ hydrogels and hyaluronidase degraded only AHA hydrogels.

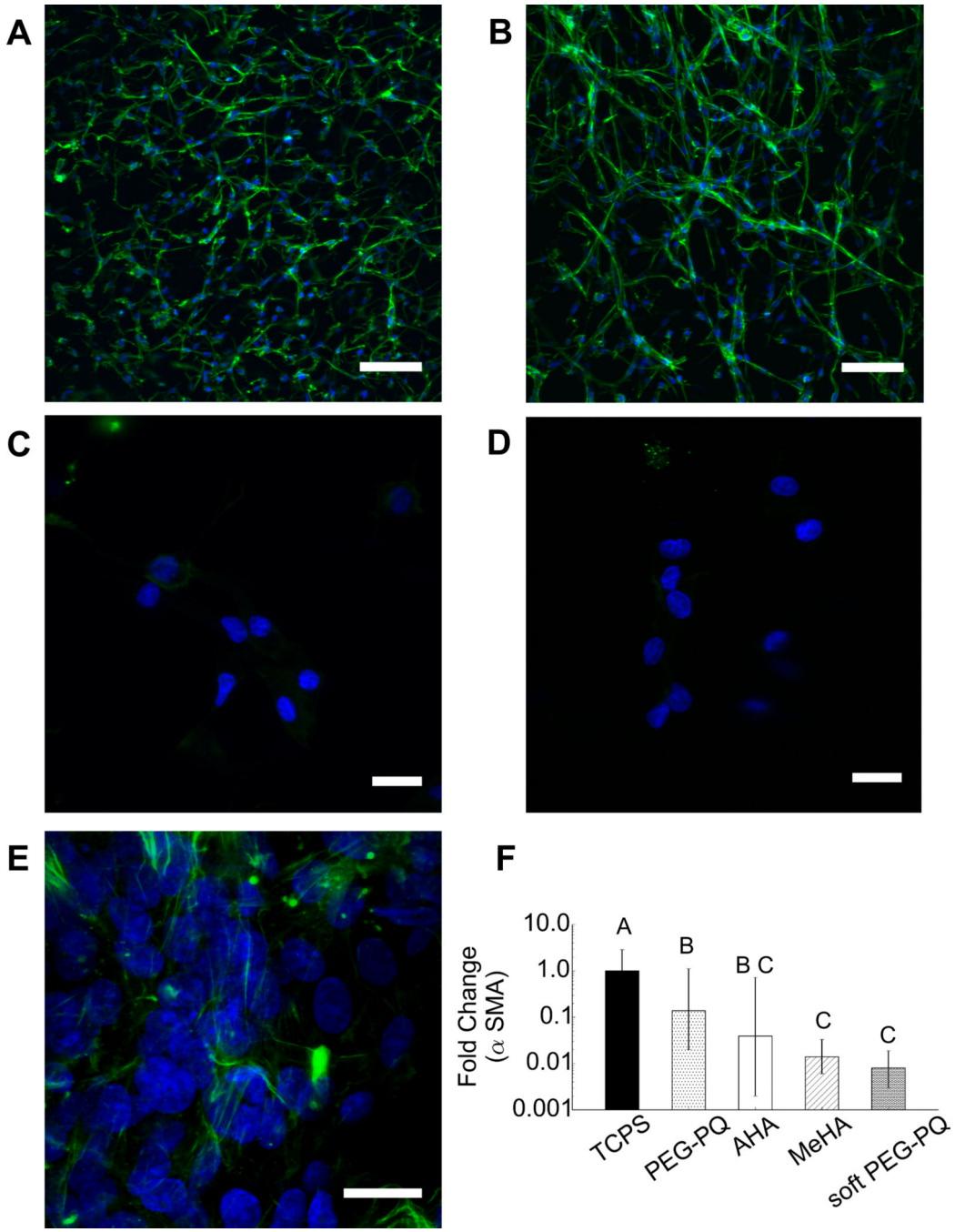

Figure 2.

(A, B) 100 μm maximum intensity z-projection of VICs encapsulated for 14 days in (A) PEG-PQ and (B) AHA hydrogels; blue = DAPI; green = F-actin; scale = 100 μm. (C, D) Faint, diffuse αSMA expression in interior of hydrogels; 30 μm maximum intensity z-projection of VICs inside (C) PEG-PQ and (D) AHA hydrogels. (E) The only strong positive staining for αSMA stress fibers was on the surface of hydrogel (15 μm maximum intensity z-projection); blue = DAPI; green = αSMA; scale = 20 μm. (F) Gene expression of αSMA; TCPS αSMA expression was significantly greater than in 3D hydrogels ($p < 0.01$); 1700

kDa MeHA αSMA expression was less than PEG-PQ ($p < 0.05$; bars that do not share a common letter are significantly different from each other).

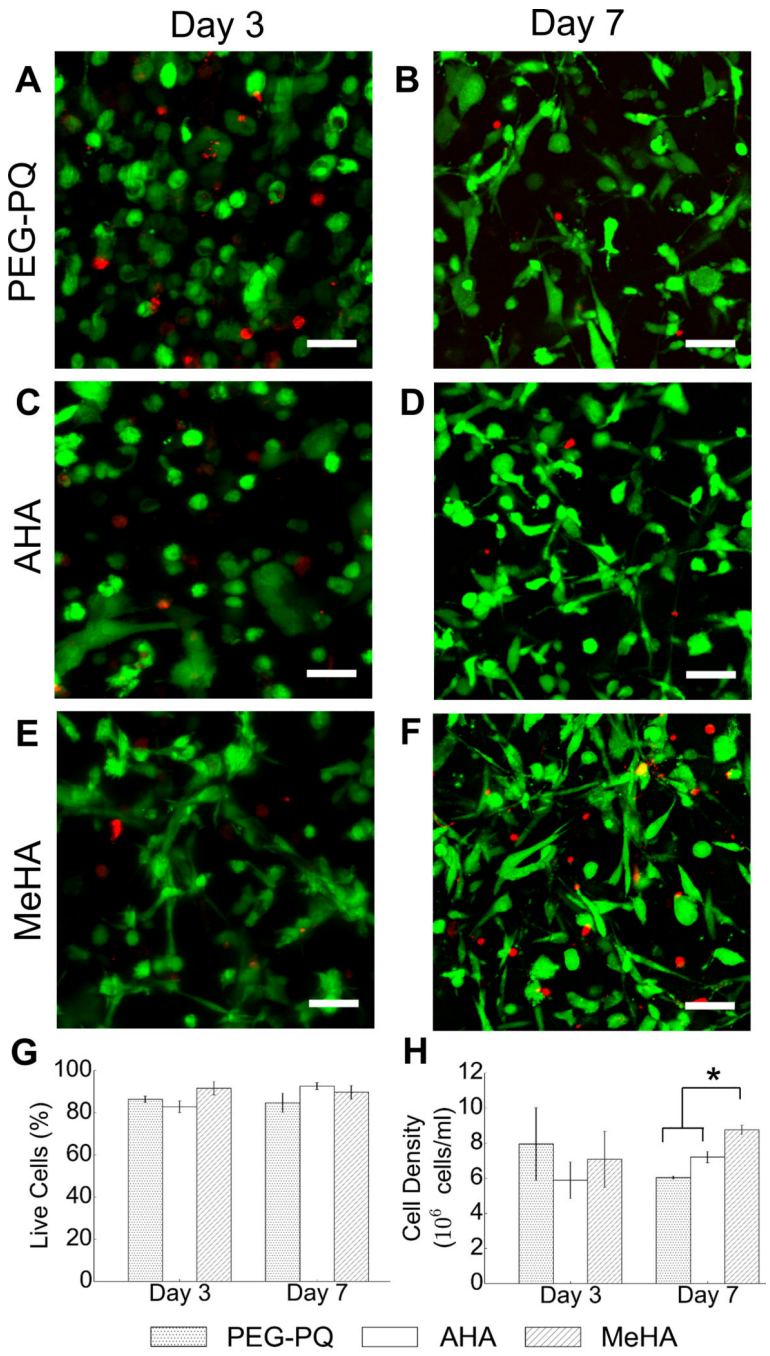

Figure 3.

Representative LIVE/DEAD staining of VICs at (A, C, E) day 3 and (B, D, F) day 7 postencapsulation. 200 μm maximum intensity z-projections of VICs encapsulated in (A, B) PEG-PQ, (C, D) AHA, and (E) MeHA hydrogels; (F) 150 μm maximum intensity z-projection in MeHA hydrogels; green = live; red = dead; scale = 50 μm. (G) Encapsulated VICs had greater than 80% viability in all hydrogel formulations. (H) Total cell density remained consistent from day 3 to day 7. At day 7, there was a significantly higher density of VICs in MeHA hydrogels than PEG-PQ and AHA hydrogels ($p < 0.05$).

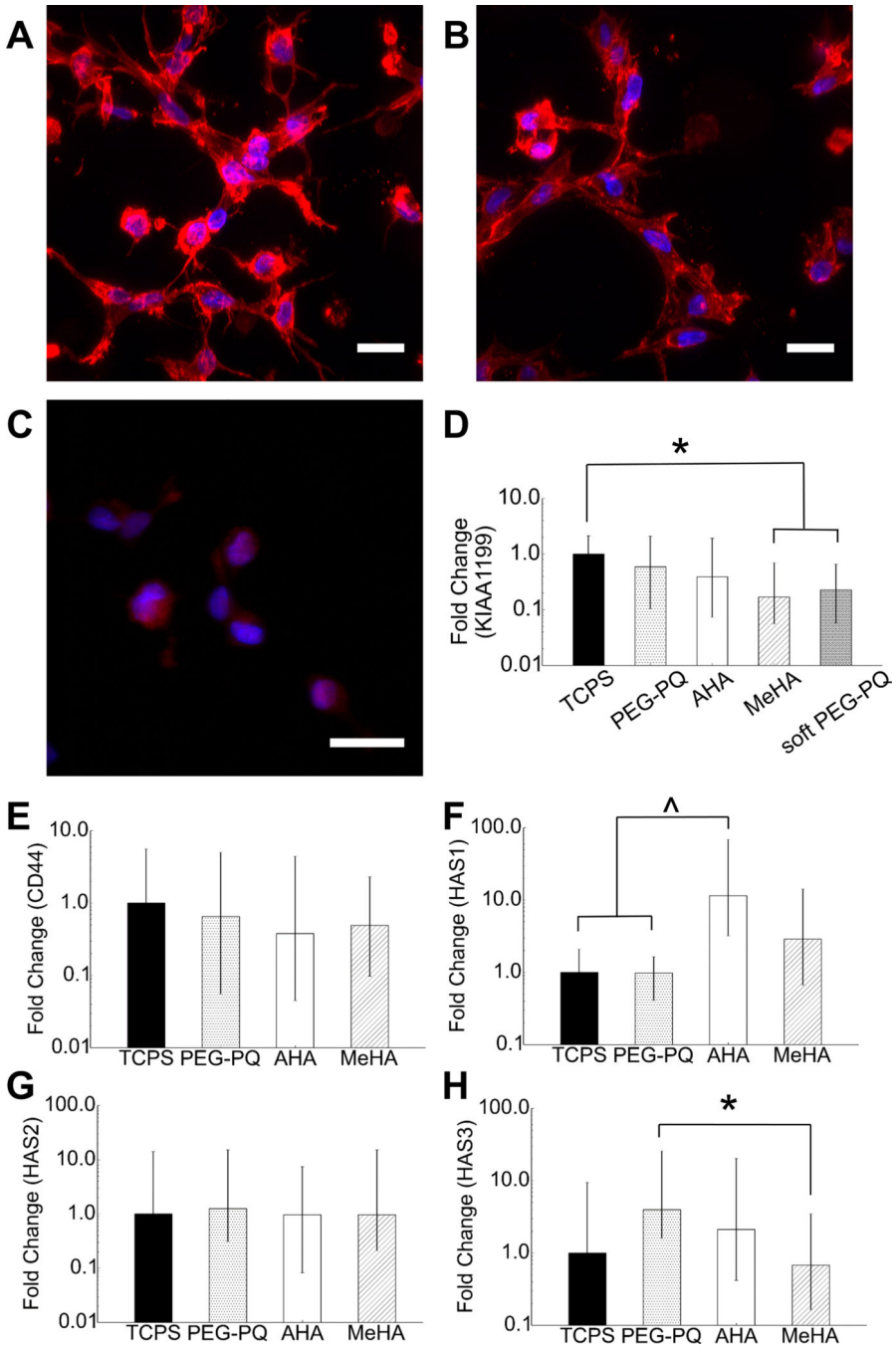

Figure 4.

After 14 days in culture, VICs in both (A) PQ and (B) AHA hydrogels showed similar, ubiquitous CD44 expression (90 μm maximum intensity z-projection); blue = DAPI; red = CD44; scale = 20 μm). (C) Only weak, diffuse intracellular RHAMM was seen in AHA hydrogels (50 μm maximum intensity z-projection); blue = DAPI; red = RHAMM; scale = 20 μm. (D) Gene expression of protein KIAA1199 in VICs grown on TCPS was significantly greater than VICs grown in 1700 kDa MeHA and soft PEG-PQ hydrogels, demonstrating that stiffness might play a role in KIAA1199 expression (*$p < 0.05$). (E–H)

CD44 and hyaluronan synthase (HAS1, HAS2, HAS3) gene expression was similar in all scaffolds, except for AHA HAS1 expression, which was significantly greater than both TCPS and PEG-PQ ($p < 0.01$). HAS3 expression was also significantly greater in PEG-PQ than MeHA ($^*p < 0.05$).

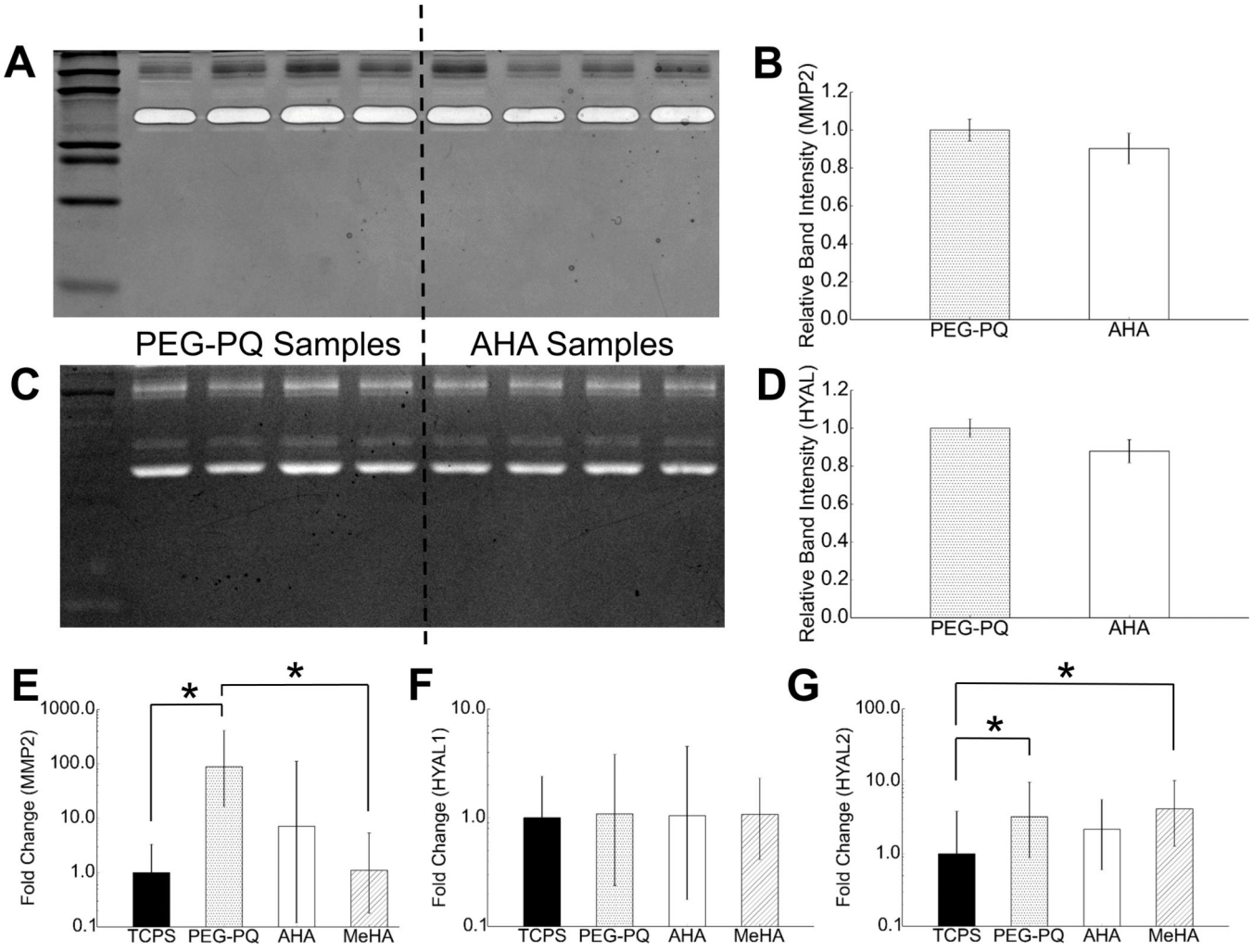

Figure 5.

Zymograms to detect enzyme activity in conditioned media. (A) Gelatin substrate zymography detects strong MMP2 activity, however, there is (B) no statistically significant difference between cells grown in PEG-PQ or AHA hydrogels. (C) Hyaluronan substrate zymography detects strongest enzyme activity (HYAL1) at just above 50 kDa; there is (D) no difference in hyaluronidase enzyme activity between cells grown in PEG-PQ or AHA hydrogels. (E–G) Gene expression of MMP2, HYAL1, and HYAL2 enzymes. (E) MMP2 expression was significantly higher in PEG-PQ hydrogels than TCPS and MeHA (*$p < 0.01$); (F) HYAL1 expression was similar in all scaffolds; (G) VICs grown on TCPS have significantly lower HYAL2 expression than VICs grown in PEG-PQ or MeHA hydrogels (*$p < 0.01$).

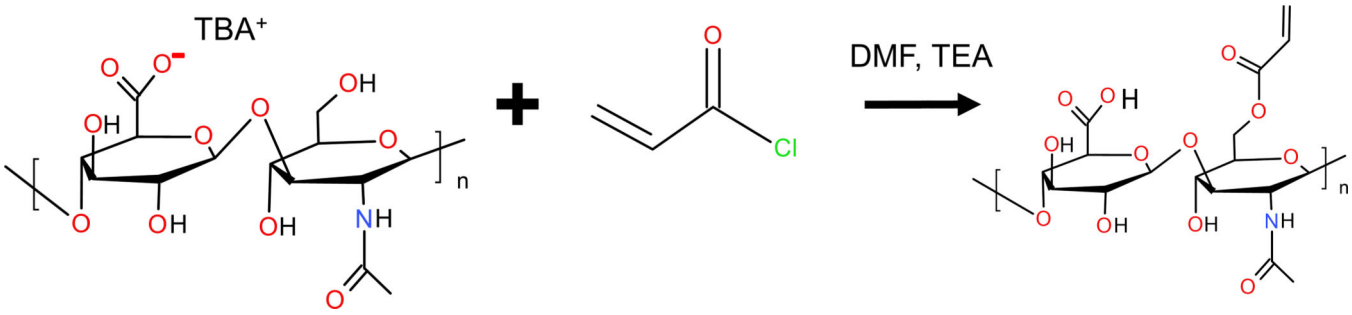

Scheme 1.

Functionalization of Hyaluronan Polymers for Free-Radical Cross-Linking with Acrylate Groups Using Acryloyl Chloride Overnight in DMF

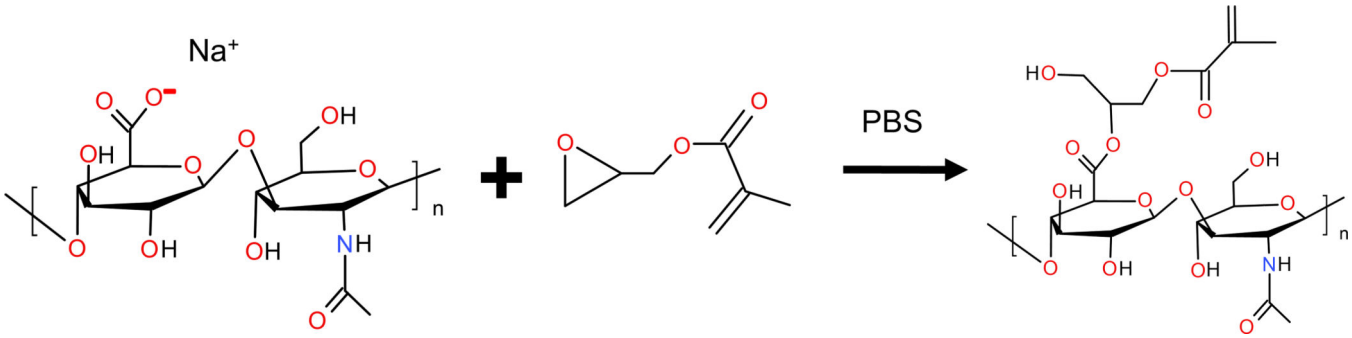

Scheme 2.

Functionalization of Hyaluronan Polymers for Free-Radical Cross-Linking with Methacrylate Groups Using Glycidyl Methacrylate for 5 Days in PBS

Table 1

Hydrogel Formulation and Resultant Mechanical Properties [a]

Polymer	DOM (%)	Density (% w/v)	X-link time (s)	Compressive modulus (kPa)	Hysteresis (%)	Volumetric swelling (%)
PEG-PQ-PEG		4	28	2.67 ± 0.12	43.1 ± 2.1	59.7 ± 2.3
soft PEG-PQ-PEG		4	22	1.46 ± 0.13	82.2 ± 2.6	54.7 ± 5.0
35 kDa AHA	7.2 ± 0.7 (n = 12)	2	25	2.66 ± 0.10	58.3 ± 1.4	70.9 ± 5.4
35 kDa MeHA	2.6 ± 0.1 (n = 2)	4	40	2.88 ± 0.16	42.8 ± 3.4	184.3 ± 6.7
1700 kDa MeHA	2.1 (n = 1)	0.75	120	1.53 ± 0.12	74.7 ± 2.1	28.4 ± 5.1

[a] Statistical comparisons of the mechanical properties are shown in Figure 1.